

## Synthesis and characterization of $\text{Ge}_x\text{Ni}_{1-x}$ composite films obtained by deposition of germanium and nickel

© N.M. Suleimanov<sup>1</sup>, A.A. Abdullina<sup>2</sup>, V.V. Bazarov<sup>1</sup>, N.M. Lyadov<sup>1</sup>, N.R. Khanov<sup>1,2</sup>, V.A. Shustov<sup>1</sup>

<sup>1</sup>Zavoisky Physical-Technical Institute, FRC Kazan Scientific Center of RAS, Kazan, Russia

<sup>2</sup>Kazan State Power Engineering University, Kazan, Russia

E-mail: vbazarov1@gmail.com

Received July 4, 2025

Revised August 20, 2025

Accepted September 1, 2025

A series of  $\text{Ge}_x\text{Ni}_{1-x}$  films were synthesized on single-crystal silicon substrates using direct-current magnetron sputtering in a high-vacuum chamber. The films were produced by simultaneous sputtering of two targets: semiconductor germanium and metallic nickel. The chemical composition of the films was studied by X-ray photoelectron spectroscopy. It has been established that thermal annealing of films leads to the formation of a nickel germanide ( $\text{NiGe}$ ) phase. Scanning electron microscopy has revealed areas that can be attributed to this phase.

**Keywords:** electrode materials, metal nanoparticles, electrocatalytic activity, semiconductor nanostructured systems.

DOI: 10.61011/TPL.2026.01.62816.20433

Composite materials based on semiconductors doped with transition metals attract significant research attention due to their magnetic properties [1,2] and the possibility of formation of metal nanoparticles, which may be catalytically active [3], in such systems. Alcohol-based (methanol and ethanol) fuel cells are currently being studied extensively. The use of metallic nickel instead of platinum or palladium to accelerate the electrooxidation of alcohols on electrode electrocatalysts may provide significant economic benefits, stimulating the search for new ways to obtain composite media with nanosized nickel inclusions. Typical materials of this kind are film structures obtained by molecular epitaxy, where ions of transition elements are localized at sites or interstitial positions in the semiconductor matrix. Theoretical calculations [4] demonstrate that atoms of transition elements in such non-equilibrium systems, where a certain fraction of atoms of the semiconductor matrix are substituted with transition element atoms or are located at interstitial sites, tend to cluster, which translates into the emergence of nanoscale formations in these structures. Germanium matrices are appealing due to the relative ease of formation of a porous coating via ion beam processing [5,6]. In the present study, we report the results of synthesis and structural examination of composite  $\text{Ge}_x\text{Ni}_{1-x}$  films obtained via deposition of semiconductor germanium and a transition 3d metal (nickel) using the method of magnetron sputtering.

A series of polycrystalline  $\text{Ge}_x\text{Ni}_{1-x}$  ( $x \geq 0.7$ ) films were synthesized on single-crystal (111) silicon substrates by DC magnetron sputtering in a high-vacuum chamber (baseline vacuum  $< 5 \cdot 10^{-7}$  Pa). These films were deposited by simultaneous sputtering of germanium (99.95 % pure) and nickel (99.99 % pure) targets. To obtain the required

composition of samples, the deposition rates of each element were calibrated. The chemical composition of films was analyzed by X-ray photoelectron spectroscopy (XPS). It was found that all films contained germanium and nickel only (the approximate sensitivity of the method is 0.5 at.%). Figure 1 shows the characteristic X-ray photoelectron emission spectra for certain samples.

Data on the concentration of elements in synthesized films are listed in the table.

X-ray phase analysis of the synthesized composite  $\text{Ge}_x\text{Ni}_{1-x}$  films was carried out using a DRON-7 setup in the Bragg–Brentano geometry. The obtained diffraction patterns were analyzed in MAUD (ver.2.999) [7,8]. Figure 2 presents the diffraction pattern of the film with the maximum nickel concentration ( $\text{Ge}_{0.7}\text{Ni}_{0.3}$ ) synthesized on a silicon substrate. The film thickness was 600 nm. The diffraction pattern features broad lines, indicating that the as-prepared films were amorphous. The results of analysis in MAUD revealed the presence of a highly disordered mixture of  $\text{Ni}_{18}\text{Ge}_{12}$  [9] and  $\text{NiGe}$  nickel germanides.

Figure 3 shows the experimental and model diffraction patterns of the  $\text{Ge}_{0.7}\text{Ni}_{0.3}$  film subjected to thermal annealing in vacuum (under a residual pressure of  $9 \cdot 10^{-4}$  Pa) at 300 °C for 15 min. It is evident that the samples subjected to thermal annealing feature narrow diffraction lines of germanium and nickel germanide  $\text{NiGe}$ , which are indicative of partial crystallization of the initially amorphous  $\text{Ge}_{0.7}\text{Ni}_{0.3}$  film after annealing. The obtained result agrees closely with the data reported in [10], where the phase evolution of the Ge/Ni system was studied at different annealing temperatures. According to MAUD data, the average size of the coherent scattering region of the  $\text{NiGe}$

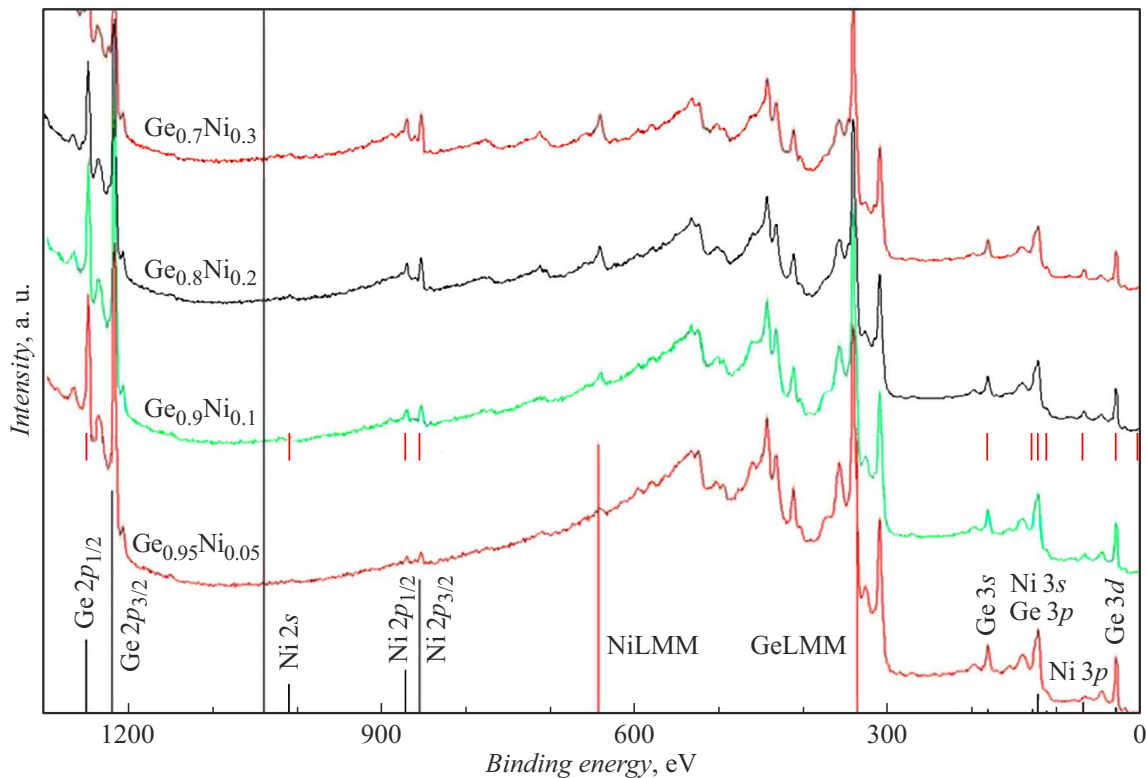


**Figure 1.** X-ray photoelectron spectra of  $Ge_xNi_{1-x}$  films of various compositions.

phase (determined by the line width) is  $\sim 400$  nm. The (111) line of the silicon substrate is also present.

The 600-nm-thick  $Ge_{0.7}Ni_{0.3}/Si$  film was imaged after deposition and after thermal annealing in vacuum with a Carl Zeiss EVO 50XVP scanning electron microscope (SEM). Figure 4 shows the surface of films after thermal annealing imaged in secondary electron (SE) and backscattered electron SEM modes. It should be taken into account that SE images reveal the morphology of the sample surface. No morphological features are seen in Fig. 4, *a*. Micrographs obtained in the backscattered electron mode in the indicated observation conditions reveal the conductive and compositional properties of the material in a layer with a thickness of approximately 50 nm. In certain cases, this is sufficient to observe metal particles in a non-conductive matrix. Imaging of the surface in the backscattered electron mode revealed the lack of charge accumulation effects. In this case, the image is formed through compositional contrast. Examining the micrograph shown in Fig. 4, *b*, one may distinguish light-colored formations 150–200 nm in size, which are clusters of the material with an increased concentration of the element with a higher atomic mass (i. e., germanium). Nickel is dominant in dark regions. We believe that the observed pattern corresponds to germanium particles immersed in the nickel germanide  $NiGe$  matrix. This conclusion is verified by the results of X-ray diffraction experiments for this film.

Nickel content determined by XPS for experimental samples of composite  $Ge_xNi_{1-x}$  films with a thickness of 600 nm synthesized by magnetron deposition of germanium and nickel on single-crystal Si (111) substrates

Sample	Nickel concentration, at. %
Ge	0
$Ge_{0.95}Ni_{0.05}$	7.7
$Ge_{0.9}Ni_{0.1}$	11.6
$Ge_{0.8}Ni_{0.2}$	20.9
$Ge_{0.7}Ni_{0.3}$	29.0

Thus, exploratory experiments on the synthesis of composite  $Ge-Ni$  films by simultaneous deposition of germanium and nickel via magnetron sputtering were carried out. X-ray photoelectron measurements, which revealed that the synthesized films contained germanium and nickel in varying concentrations, were performed. The obtained samples were examined by X-ray diffraction. The as-prepared samples contained nickel in a highly disordered mixture of germanium and nickel germanides  $Ni_{18}Ge_{12}$  and  $NiGe$ . Following 15 min of annealing at a temperature of  $300^\circ C$ , diffraction lines characteristic of germanium and nickel germanide  $NiGe$  emerged in the X-ray spectra. Electron microscopic studies revealed surface formations

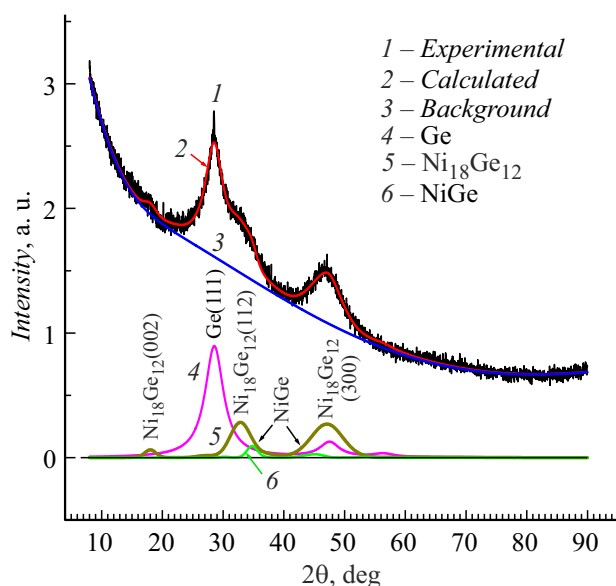


**Figure 2.** X-ray diffraction pattern for a 600-nm-thick  $\text{Ge}_{0.7}\text{Ni}_{0.3}$  film on a silicon substrate after deposition. Experimental, calculated, and background dependences are presented. Lines corresponding to amorphous germanium and  $\text{Ni}_{18}\text{Ge}_{12}$  and NiGe nickel germanides are indexed.

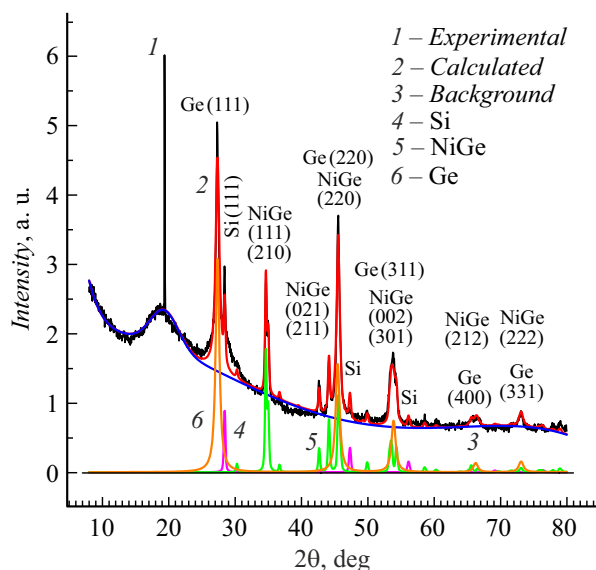


**Figure 3.** X-ray diffraction pattern for a  $\text{Ge}_{0.7}\text{Ni}_{0.3}$  film on a silicon substrate subjected to thermal annealing in vacuum at  $300\text{ }^{\circ}\text{C}$  for 15 min. Experimental, calculated, and background dependences are presented. Lines corresponding to germanium and nickel germanide NiGe are indexed.

150–200 nm in size, which may be attributed to Ge and NiGe phases, in a 50-nm-thick near-surface layer of films.

### Acknowledgments

The authors wish to thank I.V. Yanilkin for conducting experiments on synthesis of Ge–Ni intermetallic films.

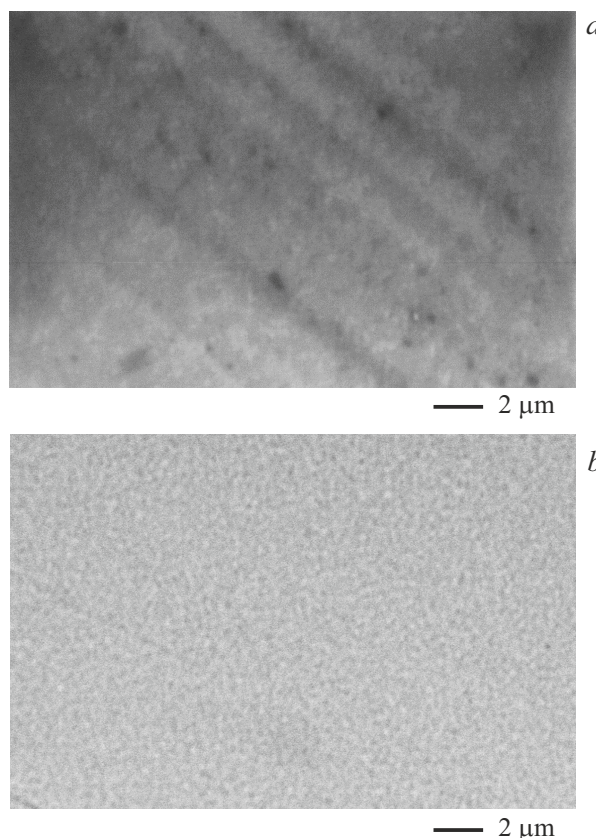


**Figure 4.** SEM images of a 600-nm-thick  $\text{Ge}_{0.7}\text{Ni}_{0.3}/\text{Si}$  film obtained in secondary electron (a) and quadrant backscatter diffraction (b) modes.

### Funding

This study was supported by a grant from the Russian Science Foundation (project No. 24-23-00544, <https://rscf.ru/project/24-23-00544/>). The synthesis and XPS analysis of films were supported by the Strategic Academic Leadership Program of the Kazan Federal University (Priority 2030).

### Conflict of interest

The authors declare that they have no conflict of interest.

### References

- [1] D. Saikia, J.P. Borah, *Appl. Phys. A*, **124**, 240 (2018). DOI: 10.1007/s00339-018-1623-4
- [2] S. Roy, M.P. Ghosh, S. Mukherjee, *Appl. Phys. A*, **127**, 451 (2021). DOI: 10.1007/s00339-021-04580-z
- [3] F. Anchieta e Silva, V.M. Martins Salim, T. Silva Rodrigues, *Appl. Chem.*, **4**, 86 (2024). DOI: 10.3390/appliedchem4010007
- [4] P. Mahadevan, J.M. Osorio-Guillén, A. Zunger, *Appl. Phys. Lett.*, **86**, 172504 (2005). DOI: 10.1063/1.1921359
- [5] V.V. Bazarov, V.A. Shustov, N.M. Lyadov, I.A. Faizrahmanov, I.V. Yanilkin, S.M. Khantimerov, R.R. Garipov, R.R. Fatykhov, N.M. Suleimanov, V.F. Valeev, *Tech. Phys. Lett.*, **45** (10), 1047 (2019). DOI: 10.1134/S1063785019100183.

- [6] N.M. Lyadov, T.P. Gavrilova, S.M. Khantimerov, V.V. Bazarov, N.M. Suleimanov, V.A. Shustov, V.I. Nuzhdin, I.V. Yanilkin, A.I. Gumarov, I.A. Faizrakhmanov, L.R. Tagirov, *Tech. Phys. Lett.*, **46** (7), 707 (2020). DOI: 10.1134/S1063785020070196.
- [7] L. Lutterotti, *Nucl. Instrum. Meth. Phys. Res. B*, **268** 334 (2010). DOI: 10.1016/j.nimb.2009.09.053
- [8] *MAUD — Materials Analysis Using Diffraction (and more)* [Electronic source]. <http://maud.radiographema.eu>
- [9] M. Kars, A.G. Herrero, T. Roisnel, A. Rebbah, L.C. Otero-Díaz, *Acta Cryst. E*, **71**, 318 (2015). DOI: 0.1107/S2056989015003680
- [10] V. Begeza, L. Rebohle, H. Stocker, *J. Alloys Compd.*, **990**, 174420 (2024). DOI: 10.1016/j.jallcom.2024.174420

*Translated by D.Safin*